Phase Matching of High-Order Harmonics in Hollow Waveguides

Charles G. Durfee III,* Andy R. Rundquist, Sterling Backus, Catherine Herne,
Margaret M. Murnane, and Henry C. Kapteyn

Center for Ultrafast Optical Science, University of Michigan, 2200 Bonisteel Boulevard, Ann Arbor, Michigan 48109-2099

(Received 9 March 1999)

We investigate the phase matching of a high-harmonic generation by intense, 20 fs laser pulses in a gas-filled capillary waveguide. We identify several regimes in which the harmonic field can build up coherently: a balance of atomic and waveguide dispersions, noncollinear Cerenkov phase matching, and a balance of atomic and plasma dispersions. The role of atomic dispersion is examined by measuring and calculating the harmonic signal for several gases. We also predict and provide preliminary evidence for a regime where phase matching occurs only at specific fractional ionization levels, where the harmonic signal is sensitive to the absolute phase of the carrier wave.

PACS numbers: 42.65.Ky, 32.80.Wr, 42.65.Re

An atom illuminated by light of ionizing intensity can radiate coherent harmonics of the incident laser that extend into the soft-x-ray region of the spectrum. While initial experiments made use of picosecond driving pulses [1,2], more recently the use of femtosecond pulses [3,4] has resulted in the generation of photon energies above 500 eV [5]. There is a wide range of applications of this source of coherent extreme ultraviolet (XUV) light in physics, chemistry, and biochemistry, and potentially in industry. In efforts to understand and improve the conversion efficiency of high-harmonic generation (HHG), attention has been paid to the fundamental laser-atom interaction as well as the macroscopic phase-matching effects that control the buildup of the harmonic signal over the interaction length [6]. In the typical experimental geometry, where an intense pulse is focused into a gas jet, phase matching is dominated by the relative phase shifts of the fields as they pass through the focus (i.e., the Guoy phase shift) [7,8]. While some enhancement comes from positioning the interaction region after the focus of the beam [9], the divergence of the laser beam either limits the interaction length or requires a large confocal parameter (and large laser energy) to implement efficiently. In recent work, we demonstrated that this limitation could be circumvented by generating high harmonics with submillijoule energy ultrashort light pulses guided in a gas-filled capillary waveguide [10]. The plane-wave nature of the mode makes it possible to balance, over an extended interaction length, the anomalous dispersion of the neutral gas with the normal dispersion of the waveguide and the free electrons [11]. In this paper, we report on several new experimental results along with a model that sheds light on the physical mechanisms involved in the phase matching. We investigate the dependence of the phase-matching process on gas species and absorption of the harmonic signal. It has not been recognized previously that even in the absence of a waveguide, neutral gas dispersion can play an important role in the observed HHG conversion efficiency. The calculations reveal that confinement of the fundamental mode in the waveguide allows phase matching at a higher ionization fraction than would be expected from a 1D plane-wave analysis. We show three limiting regimes of phase matching: a balance between the neutral gas and the waveguide dispersion, the neutral gas and the plasma dispersion, and Cerenkov (noncollinear) phase matching. In the second of these regimes, we predict that phase matching occurs only at specific ionization fractions, leading to an output signal that is sensitive to the absolute phase of the carrier wave with respect to the pulse envelope.

The propagation constant, k_f, for the fundamental traveling in the lowest mode of a step-index waveguide of radius a filled with a medium of refractive index n, is given by $k_f^2 = n^2 k_0^2 - (u_{11}/a)^2$. Here k_0 is the vacuum wave number and $u_{11} = 2.405$ is the first zero of the Bessel function J_0 [12]. For a partially ionized gas we can write $n = 1 + P[(1 - \eta)\delta(\lambda) - \eta N_{\text{atm}} r_e \lambda^2/2\pi + (1 - \eta)n_2 I]$, where P, η, N_{atm}, $\delta(\lambda)$, r_e, n_2, and I represent the pressure in atmospheres, the ionization fraction, the number density at one atmosphere, the neutral gas dispersion, the classical electron radius, the nonlinear refractive index, and the pulse intensity, respectively. This gives the following propagation constant:

$$k \approx \frac{2\pi}{\lambda} + \frac{2\pi P(1 - \eta)\delta(\lambda)}{\lambda} + (1 - \eta)n_2 I - P\eta N_{\text{atm}} r_e \lambda - \frac{u_{11}^2 \lambda}{4\pi a^2}, \quad (1)$$

where the terms on the right correspond to the respective contributions from vacuum, neutral gas dispersion, nonlinear refractive index, plasma dispersion, and waveguide dispersion. We neglect the x-ray modal contribution: the harmonic light has a confocal parameter much longer than the capillary lengths considered here and does not encounter the capillary walls.

Since ionization is localized near the optical axis, only a portion of the fundamental mode propagates through the plasma. Provided the plasma density is sufficiently small, the shape of the guided mode field is not greatly affected. In this regime, the radial variations in the refractive index may be treated as a perturbation, in a

similar approach to that taken with self-phase modulation in optical fibers [13]. To reduce computation, we calculate an effective index by averaging $n(r)$ over the fundamental mode. We compared this method with another in which the radial wave equation is solved for the new mode, and we found that the approximation is accurate in regimes of low density and/or low ionization fraction. This modal averaging reduces the effect of the plasma density by as much as a factor of 5, and allows phase matching of higher-order harmonics than could normally occur with plane waves. We retain the nonlinear index in the calculations, but its effect is small: in argon, $n_2 I$ is only about 7% of the linear component $N_a \delta$ at an intensity of 2×10^{14} W/cm^2 (using a value of $n_2 = 9.8 \times 10^{-24}$ cm^2/W at 1 bar [14]—a possible overestimate by $\sim 4\times$ [15]).

The phase mismatch for the qth harmonic generation $\Delta k = k_q - q k_f = q k_0 [n(\lambda_q) - n(\lambda_0)]$, or

$$\Delta k \approx q \frac{u_{11}^2 \lambda_0}{4\pi a^2} + N_e r_e (q\lambda_0 - \lambda_q) - \frac{2\pi N_a}{\lambda_q} [\delta(\lambda_0) - \delta(\lambda_q)], \quad (2)$$

where the nonlinear index term has been omitted. The growth of the harmonic in the presence of absorption by the medium is modeled here by

$$|E|^2 \approx N_a^2 |\chi_{\text{eff}}^{(q)} E_0^s|^2 \left(\frac{1 + e^{-2\alpha L} - 2e^{-\alpha L} \cos \Delta k L}{\alpha^2 + \Delta k^2} \right), \quad (3)$$

which reduces to the familiar $\text{sinc}^2(\Delta k L/2)$ dependence [where $\text{sinc}(x) = \sin(x)/x$] for a field absorption coefficient of $\alpha = 0$. In this simple model the nonlinear source term has an effective field dependence of order $s \sim 5$ [8]. The important physical consequence of Eq. (3) is that the signal strength is determined by the shorter of the coherence length $(1/\Delta k)$ and the absorption depth $(1/2\alpha)$. The strong absorption of gases for photon energies greater than the ionization potential therefore dominates the yield that can be obtained at different harmonics [16,17]. This limitation can be circumvented by the use of short pump pulses (presented here), the use of wave-mixing schemes [18], or more complicated geometries [19], to operate in the transparency regions of the various gases.

Our experimental setup has been described elsewhere [10]. Briefly, laser pulses from a kilohertz Ti:sapphire multipass amplifier ($<$4.5 mJ, 20 fs, 800 nm) [20] were focused into a 150 μm inner-diameter capillary waveguide, with careful attention to mode matching of the beam to the lowest spatial mode. A three-segment capillary tube (6.3 mm outer diameter) was used for these experiments, which allowed us to produce a constant pressure region within the center section (3 cm), while the end sections (1.7 cm) exited to vacuum [10,16]. We performed a series of measurements that explores different regimes of phases matching. In the first, low intensity regime, there is very little ionization, and phase matching occurs primarily as a balance of the dispersion of the neutral atoms and the waveguide. Figure 1(a) shows the dependence of the harmonic signal (19th, 21st, 23rd) on the pressure of argon in the center capillary section, at an intensity of 1.2×10^{14} W/cm^2 (140 μJ, 23 fs). At this intensity, the cutoff harmonic is the 25th, and the ionization fraction at the peak of the pulse is 0.5%. Conversion within the central, constant density section of the cell results in the low-pressure peak near 15 Torr, as predicted by theory. As the gas accelerates into the end section the pressure drops by $\sim 3\times$ then decreases further along the way to the exit [21]. Conversion within this last section of the capillary cell gives the higher pressure and broader secondary peaks at cell pressures that yield the optimum of $\sim$15–20 Torr somewhere within the gradient.

For harmonics 19–23, the signal is strongly absorbed by the neutral argon [Fig. 1(b), dashed line]. Increasing the intensity allows higher-harmonic orders where the gas transmission is greater [Fig. 1(b), solid line]. Here the signal from the end section is dominated by that from the center, where the constant pressure allows a phase-matched signal to build up over a longer distance, giving a high conversion efficiency. This harmonic spectrum is in sharp contrast to the usual plateau of harmonics, and shows clearly that the phase matching allows the signal strength to be limited by the absorption depth.

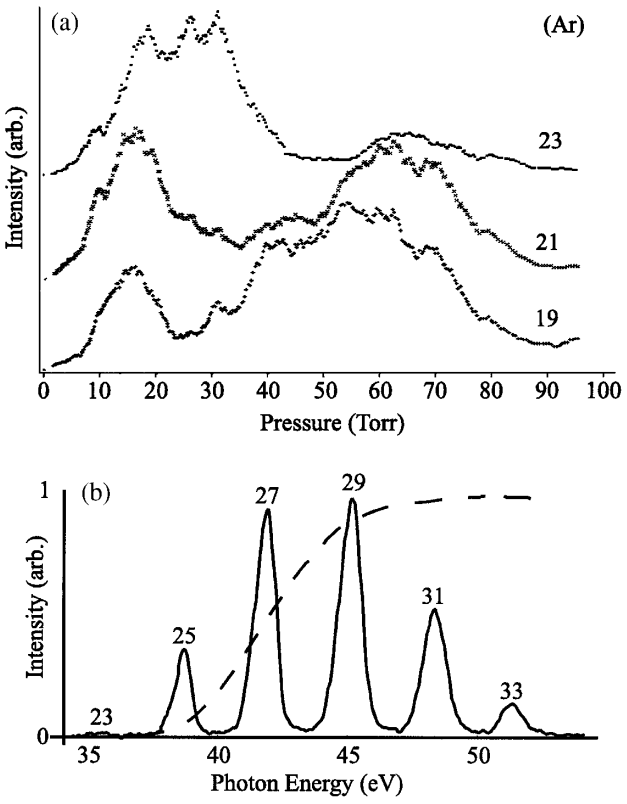

FIG. 1. (a) Pressure dependence of the signal for harmonics 19, 21, and 23 generated in argon at a peak intensity of 1.2×10^{14} W/cm^2. (b) Harmonic spectrum at 1.8×10^{14} W/cm^2 (solid line) and the calculated transmission of 5 mm neutral argon at 30 Torr.

We further explored the interplay of the neutral and plasma dispersion by measuring the pressure dependence of the harmonic signal for several gases—Xe (23rd harmonic), Kr (25th), Ar (29th), and H_2 (25th) [Fig. 2(a)]. The more dispersive the gas, the lower the optimum pressure for phase matching, since a lower gas density is required to match the dispersion of the waveguide and free electrons generated from ionization. The higher fractional ionization here places these experiments in a transitional regime, where the dispersive contributions of the waveguide and plasma are equally important. The increase in η requires an increase in pressure to maintain phase matching [see Eq. (2)]. The temporal dependence of the ionization level broadens and increases the phase-matching pressure peak. In our calculations to model this regime [see Fig. 2(b)], we first compute the fractional ionization profile $\eta(r,t)$ using the ADK tunneling ionization rates [22], and then use the modal averaging to calculate the effective refractive index for each temporal slice of the fundamental. The harmonic light is generated and propagates in the ionized regions, so it sees the full level of ionization. There is very good agreement between the widths and locations of the pressure peaks to those found experimentally. The only fitting required was to adjust the incident intensity downward (by 15%–30%) so that ionization did not dominate the phase matching. This would be experimentally consistent with a slight defocusing of the guided beam. Other uncertainties in the calculation are the exact refractive index of the harmonic and the ionization rate. We estimate that at the peak of the pulse η was ~6% (Xe and Kr), ~8% (Ar), and 2.6% (H_2).

Still higher intensity results in another regime of phase matching that is dominated by the plasma dispersion. At a critical ionization fraction, η_{cr}, dependent on the gas species, the dispersions of neutral atoms and free electrons balance [16]. For plane-wave propagation in Ar and Xe, $\eta_{cr} = 4.8\%$ and 11%, respectively. Optimum phase matching is limited to those harmonics that can be generated with ionization levels $< \eta_{cr}$. This is mitigated by the modal averaging of the refractive index (which results in much higher values of η_{cr}) and the short input pulse duration, which allows atoms to experience higher intensity at a given level of ionization [4]. The rapid variation of the instantaneous intensity that results from the oscillations at the carrier frequency leads to incremental increases in η at each half-cycle of the field. As η approaches η_{cr}, each of these steps should have a distinct optimum pressure [Fig. 3(a)]. The location of these peaks is sensitive to the phase of the carrier with respect to the pulse envelope. The lack of experimental control over this absolute phase leads to rapid fluctuations in the yield at high pressures [Fig. 3(b)]. As $\Delta k \sim 0$ only for a small time period within a single cycle of the driving field, this absolute phase effect may provide a method of generating efficient attosecond-duration XUV pulses from the guided wave geometry.

The spatial profile of the phase-matched harmonic emission was recorded with a microchannel plate 0.68 m from the exit of the capillary. An aluminum filter blocked the fundamental and low orders (<11). The images represent the signal primarily from a few orders near the 29th [see Fig. 1(b) and discussion]. The spot size is largest at low pressure [Fig. 4(a), 10 Torr], and decreases at higher pressure [Fig. 4(b), 20 Torr], until, at the phase-matched pressure [Fig. 4(c), 45 Torr], a well-defined output mode is observed. At still higher pressures, the signal strength decreases without much change in output spot size. This evolution in spatial mode of the XUV light at low pressure demonstrates a third regime of noncollinear phase matching. At low pressure, the positive phase mismatch from

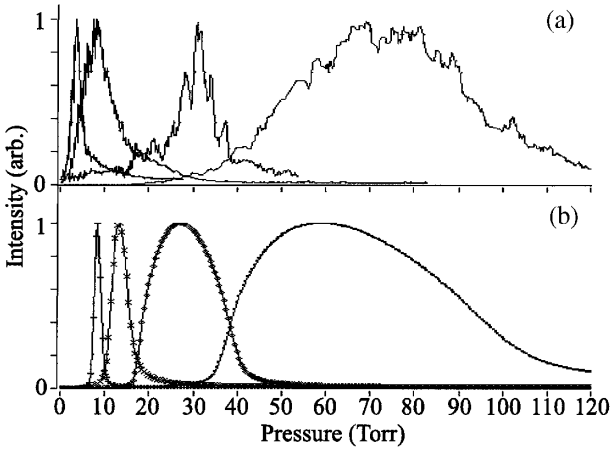

FIG. 2. Measured (a) and calculated (b) pressure dependence of the harmonic yield for several gases. In order of increasing optimum pressure, the curves correspond to xenon, krypton, argon, and hydrogen.

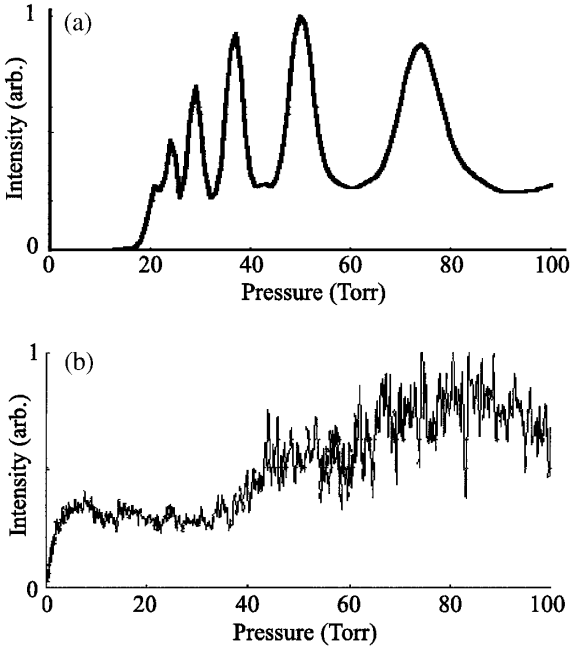

FIG. 3. (a) Calculated pressure dependence of the yield of harmonic 29 for high intensity (2.2×10^{14} W/cm^2) in argon. (b) Measured signal at an incident intensity of 4×10^{14} W/cm^2.

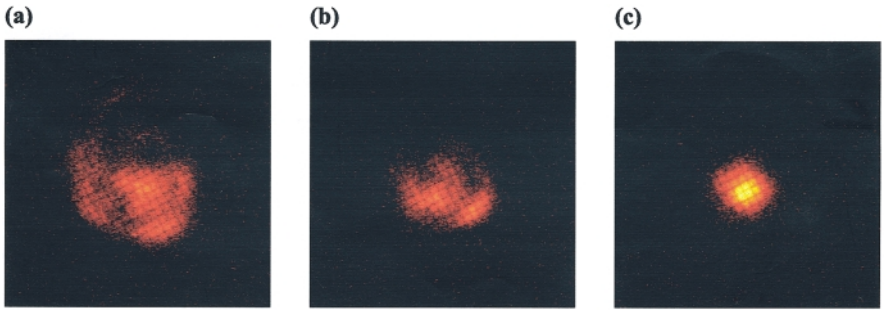

FIG. 4 (color). (a)–(c): Spatial profiles of the harmonic yield at 10, 20, and 45 Torr. The dark grid results from the mesh used to support the 0.2 mm Al filter (70 lines/in.).

the normally dispersive waveguide and plasma terms can be compensated if the harmonic emission occurs at an angle θ to the fundamental: $\Delta k = k_q \cos\theta - q k_f$. This type of phase matching is sometimes referred to as Cerenkov phase matching, since the phase velocity of the nonlinear polarization travels faster than the phase velocity of the harmonic in the medium. The maximum angle of emission $\theta_{\max}$ corresponds to the largest Δk, in this case where η is the highest. The decrease in $\theta_{\max}$ with pressure measured experimentally is in good agreement with that calculated for harmonic 29 (there is little variation for the nearby orders) and a constant value of $\eta = 11\%$, consistent with our other calculations. As Δk approaches zero, the output beam is limited in size by the diffraction-limited divergence of the mode. At higher pressures, the beam approximately maintains this divergence but the signal strength decreases. Here $\Delta k < 0$ for high pressures, and Δk would not be decreased for emission at large angles. While angular emission of HHG has been observed previously in a gas jet experiment [23], we show here for the first time the transition from off axis to axial phase matching. Note that Cerenkov phase matching is not as efficient as phase matching in the forward direction, since the signal can coherently build up only over a comparatively short distance before it leaves the source region.

We have explored several new regimes of phase matching for guided-wave high-order harmonic generation. Through careful comparison of our measurements with a simple propagation model, we have demonstrated the influence of the waveguide and gas dispersions, ionization, carrier phase, and geometry on phase matching. By controlling the gas species, ionization level, and gas pressure, phase matching was achieved over several cm lengths in Xe, Kr, Ar, and H_2 gases. Harmonic orders 17–45 have been phase matched (26–70 eV). This harmonic emission is predicted to occur over an extremely short time period of ~5 fs [24]. At the highest orders, the efficiency is limited by strong ionization. The most simple and efficient regime to achieve phase matching corresponds to a balance between the dispersion of the neutral atoms and that of the waveguide and plasma. The ultrashort pulse duration (~20 fs) allows atoms to experience high levels of intensity prior to ionization [4,5], and makes possible the generation of harmonics at energies within the transmission window of the gas while maintaining a sufficiently low ionization fraction to support phase matching. Finally, we predict a new regime in which phase matching at a given pressure occurs only at specific ionization levels, leading to an harmonic signal that is sensitive to the absolute phase of the carrier wave. This may allow very precise control over the temporal profile of the generated HHG signal.

The authors gratefully acknowledge funding for this work from the National Science Foundation.

*Email address: cdurfee@mines.edu

[1] A. McPherson *et al.*, J. Opt. Soc. Am. B **4**, 595 (1987).
[2] A. L'Huillier *et al.*, J. Phys. B **24**, 3315 (1991).
[3] J. J. Macklin, J. D. Kmetec, and C. L. Gordon III, Phys. Rev. Lett. **70**, 766 (1993).
[4] J. Zhou *et al.*, Phys. Rev. Lett. **76**, 752 (1996).
[5] Z. Chang *et al.*, Phys. Rev. Lett. **79**, 2967 (1997); C. Speilmann *et al.*, Science **278**, 661 (1997).
[6] V. T. Platonenko and V. V. Strelkov, Quantum Electron. **28**, 564 (1998).
[7] A. L'Huillier *et al.*, J. Opt. Soc. Am. B **7**, 527 (1990).
[8] A. L'Huillier *et al.*, Phys. Rev. Lett. **66**, 2200 (1991).
[9] A. L'Huillier and P. Balcou, Phys. Rev. Lett. **70**, 774 (1993).
[10] A. Rundquist *et al.*, Science **280**, 1412 (1998).
[11] C. G. Durfee *et al.*, Opt. Lett. **22**, 1565 (1997).
[12] E. A. J. Marcatili and R. A. Schmeltzer, Bell Syst. Tech. J. **43**, 1783 (1964).
[13] G. P. Agrawal, *Nonlinear Fiber Optics* (Academic Press, San Diego, 1995), 2nd ed.
[14] H. J. Lehmeier *et al.*, Opt. Commun. **56**, 67 (1985).
[15] M. Nisoli *et al.*, Opt. Lett. **22**, 522 (1997).
[16] A. Rundquist, Ph.D. thesis, Washington State University, Pullman, 1998.
[17] E. Constant *et al.*, Phys. Rev. Lett. **82**, 1668 (1999).
[18] P. L. Shkolnikov *et al.*, Opt. Lett. **18**, 1700 (1993); H. Milchberg *et al.*, Phys. Rev. Lett. **75**, 2494 (1995).
[19] I. P. Christov *et al.*, Opt. Expr. **3**, 360 (1998).
[20] S. Backus *et al.*, Opt. Lett. **22**, 1256 (1997).
[21] D. J. Santeler, J. Vac. Sci. Technol. A **4**, 348 (1986).
[22] M. V. Ammosov *et al.*, Sov. Phys. JETP **64**, 1191 (1986).
[23] P. Salieres *et al.*, J. Phys. B **29**, 4771 (1996).
[24] I. P. Christov *et al.*, Phys. Rev. Lett. **78**, 1251 (1997).